



THE UNIVERSITY *of* EDINBURGH

Edinburgh Research Explorer

Dispersive shock waves in nematic liquid crystals

Citation for published version:

Smyth, N 2016, 'Dispersive shock waves in nematic liquid crystals', *Physica D: Nonlinear Phenomena*, vol. 333, pp. 301-309. <https://doi.org/10.1016/j.physd.2015.08.006>

Digital Object Identifier (DOI):

[10.1016/j.physd.2015.08.006](https://doi.org/10.1016/j.physd.2015.08.006)

Link:

[Link to publication record in Edinburgh Research Explorer](#)

Document Version:

Peer reviewed version

Published In:

Physica D: Nonlinear Phenomena

General rights

Copyright for the publications made accessible via the Edinburgh Research Explorer is retained by the author(s) and / or other copyright owners and it is a condition of accessing these publications that users recognise and abide by the legal requirements associated with these rights.

Take down policy

The University of Edinburgh has made every reasonable effort to ensure that Edinburgh Research Explorer content complies with UK legislation. If you believe that the public display of this file breaches copyright please contact openaccess@ed.ac.uk providing details, and we will remove access to the work immediately and investigate your claim.



Dispersive shock waves in nematic liquid crystals

Noel F. Smyth^{a,*}

^a*School of Mathematics, University of Edinburgh,
Edinburgh EH9 3FD, Scotland, U.K.*

Abstract

The propagation of coherent light with an initial step intensity profile in a nematic liquid crystal is studied using modulation theory. The propagation of light in a nematic liquid crystal is governed by a coupled system consisting of a nonlinear Schrödinger equation for the light beam and an elliptic equation for the medium response. In general, the intensity step breaks up into a dispersive shock wave, or undular bore, and an expansion fan. In the experimental parameter regime for which the nematic response is highly nonlocal, this nematic bore is found to differ substantially from the standard defocusing nonlinear Schrödinger equation structure due to the effect of the nonlocality of the nematic medium. It is found that the undular bore is of Korteweg-de Vries equation-type, consisting of bright waves, rather than of nonlinear Schrödinger equation-type, consisting of dark waves. In addition, ahead of this Korteweg-de Vries bore there can be a uniform wavetrain with a short front which brings the solution down to the initial level ahead. It is found that this uniform wavetrain does not exist if the initial jump is below a critical value. Analytical solutions for the various parts of the nematic bore are found, with emphasis on the role of the nonlocality of the nematic medium in shaping this structure. Excellent agreement between full numerical solutions of the governing nematic equations and these analytical solutions is found.

Keywords: Modulation theory; Dispersive shock wave; Undular bore; Liquid crystals; Nematicon

1. Introduction

Solitary waves, or solitons for integrable equations, are thought of as the defining solution of many nonlinear wave equations, such as the Korteweg-de Vries (KdV) equation, the nonlinear Schrödinger (NLS) equation and the Sine-Gordon equation [1]. However, such equations also possess a generic solution which is just as characteristic as the soliton solution, which arises in many applications and is just as widely observed. This solution is the undular bore, or dispersive shock wave. The term undular bore arises from their first observation as wave structures in fluids and as this is the first name applied, it will be used in this work, rather than the term dispersive shock wave. For nonlinear waves

*Corresponding author
Email address: N.Smyth@ed.ac.uk (Noel F. Smyth)

governed by dispersive equations, undular bores arise when an initial jump, or near jump, linking two levels is smoothed by the action of dispersion, resulting in a smooth wavetrain linking these two levels. The generic structure of an undular bore is that it has one edge consisting of solitary waves with the opposite edge consisting of linear, dispersive waves. An undular bore is the dispersive equivalent of a gas dynamic shock, for which viscous effects smooth out the jump [1], as opposed to the dispersive effects smoothing out an undular bore. For this reason, an undular bore is also termed a dispersive shock wave. An undular bore is a non-steady wavetrain which continually expands in length. It should be noted that there is another, steady bore arising in water wave theory, a viscous bore [1, 2]. This bore is steady due to the effect of viscosity. This work will deal with undular bores in a nonlinear optical system, for which there is no equivalent of fluid viscosity. Therefore, the bores dealt with in the present work are all undular bores.

As a viscous bore is steady, it is relatively straightforward to obtain a solution for it [3]. The unsteady nature of an undular bore made finding a solution for it more difficult. Whitham [1, 4–6] developed modulation theory, or the method of averaged Lagrangians, as a method to analyse dispersive wavetrains slowly varying in both space and time. This method is related to the method of multiple scales in perturbation theory [7]. In particular, Whitham derived the modulation equations for the KdV equation [1, 5]. As the periodic (cnoidal) wave solutions of the KdV equation are stable, these modulation equations form a hyperbolic system for the parameters of the modulated cnoidal wave. Furthermore, these modulation equations could be set in Riemann invariant form. It was subsequently realised that a simple wave solution of these hyperbolic modulation equations corresponds to an undular bore solution of the KdV equation [8, 9]. A major advance occurred when it was shown using functional analysis that the ability to set the modulation equations for the KdV equation in Riemann invariant form was linked to the KdV equation having an inverse scattering solution [10], which meant that it was then clear how to calculate the modulation equations for other nonlinear dispersive wave equations having an inverse scattering solution. As few nonlinear dispersive wave equations have an inverse scattering solution, the utility of using Whitham modulation theory to find undular bore solutions of nonlinear dispersive wave equations was greatly extended when a method was found to determine the leading and trailing edges of an undular bore in the absence of the full modulation equations and for equations for which there is no inverse scattering solution to enable the modulation equations to be found using standard techniques [11, 12]. Bore solutions for a variety of nonlinear dispersive equations have now found use in a wide range of physical applications, for example water waves [13–15], oceanography [16], meteorology [17–19], geophysics [20–23] and nonlinear optics [24–28].

The present work is concerned with determining the undular bore solution for the equations governing a specific class of nonlinear optical media, the nematic liquid crystal [29–31] in the defocusing regime [32] for the usual experimental parameter range. Nematic liquid crystals are a nonlinear optical medium which support solitary waves [30, 31, 33], termed nematicons. They are usually a focussing medium, so that the nematicons are bright waves and the resulting modulation equations for the nematic equations are elliptic and so do not have an undular bore solution. However, nematic liquid crystals can be made defocusing through the addition of azo-dyes [32]. The original applications of undular bores were in fluid mechanics and water waves, hence their name, but they have recently found extensive application in nonlinear optics. Both ex-

perimental and numerical investigations have shown that undular bores can be generated in thermal nonlinear optical media [34–37] and nonlinear crystals [38, 39], among other defocusing nonlinear optical media. As these undular bores form in defocusing media, the bores are dark bores, that is dips in a background carrier wave. Nematic liquid crystals are termed nonlocal media as in the usual experimental regime the elastic response of the nematic to an optical beam extends far beyond the beam [30, 31]. While structures with some resemblance to undular bores can form in focussing nonlinear optical media [34, 39], such as nematic liquid crystals, and some approximate analytical theory has been developed for these [40, 41], there has been no theory developed for undular bores in defocusing nonlinear, nonlocal media, such as nematic liquid crystals and thermal media, which is valid for experimental parameter ranges. In this context the equations governing nonlinear beams in defocusing thermal nonlinear media [34–37] are the same as those governing nonlinear beams in defocusing nematic liquid crystals [30, 31]. In the so-called local limit the equations for optical beams in a nematic liquid crystal reduce to the standard NLS equation, for which there is a known undular bore solution [42], but, as stated, this is not the usual experimental regime.

In the present work, the undular bore solution for the equations governing nonlinear optical beam propagation in a defocusing nematic liquid crystal will be developed. It is found that the undular bore is of KdV-type, even though the equation governing the electric field of the light beam is of NLS-type. The bore then consists of bright waves, rises above a background level, rather than the dark waves, dips in a background level, of a defocusing NLS bore [42]. The method of El [11, 12] is used to show the non-existence of an NLS-type bore in the nonlocal limit. For an initial light intensity jump above a critical height, ahead of the KdV bore is a uniform wavetrain with a short front which brings the solution down to the initial level ahead. This wavetrain is generated by a phase mismatch between the KdV bore and the initial state. A phase and group velocity argument is used to find the leading and trailing edges of this uniform wavetrain. This argument predicts a minimum jump height for the uniform wavetrain to exist, which is confirmed by numerical solutions. Outside of the KdV bore and uniform wavetrain regions, the solution is given by the non-dispersive limit of the nematic equations. These various parts of the analytical solution for the nematic bore are compared with full numerical solutions of the governing equations and good to excellent agreement is found, depending on the initial jump height.

Previous experimental [34] and numerical [34–37] studies of undular bores in defocusing nonlinear, nonlocal thermal media were for $O(1)$ or $O(10)$ values of the nonlocality parameter, and so were not in the highly nonlocal regime typical of nematic liquid crystals for which the nonlocality parameter is $O(100)$, and were generated by gradient catastrophes of finite initial conditions. True undular bores cannot be generated from a finite initial condition as true bores require the continual generation of waves as the bore spreads. Breaking finite initial conditions give an approximation to an undular bore for finite propagation distances as the inverse scattering solution of the NLS equation, both focussing and defocusing, shows that a finite initial condition generates a finite number of solitons plus dispersive radiation [1]. However, some of these experimental and numerical results show evidence of the KdV-bore type structure found in the present work [34, 36], as will be discussed in more detail below.

2. Dark nematicon equations

Let us consider the propagation of polarised coherent light through a cell filled with a nematic liquid crystal. The light is taken to propagate in the z direction and the x direction is taken as the direction of polarisation of the electric field of the light. The light beam is taken to be $(1 + 1)$ dimensional, which is a valid approximation for light in a nematic liquid crystal cell due to the widely different aspect ratios of the cell in the directions transverse to propagation [44]. To overcome the optical Freédericksz threshold [29], an external low frequency electric field is applied in the polarisation direction to pre-tilt the nematic molecules [33]. With this pre-tilting field, optical solitary waves in the nematic liquid crystal, termed nematicons [30, 31], and other nonlinear optical waves can be formed with milliwatt power beams. If the beam power is high, undesirable physical effects can occur, even to the extent of the nematic phase becoming unstable [33]. Nematic liquid crystals usually form a focussing medium, so that they support bright optical solitary waves, bright nematicons [30, 31]. However, a nematic liquid crystal can become a defocusing medium through the addition of azo-dyes [32], so that dark optical solitary waves, dark nematicons, can be supported. In the paraxial, slowly varying envelope approximation, the non-dimensional equations governing the propagation of the optical beam through the defocusing nematic liquid crystal are [30–32, 45]

$$i\frac{\partial u}{\partial z} + \frac{1}{2}\frac{\partial^2 u}{\partial x^2} - 2\theta u = 0, \quad (1)$$

$$\nu\frac{\partial^2 \theta}{\partial x^2} - 2q\theta = -2|u|^2. \quad (2)$$

Here, u is the complex valued envelope of the electric field of the light and θ is the extra rotation of the nematic molecules from their pre-tilt value due to the light beam. The parameter ν measures the elasticity of the nematic and is usually large, $O(100)$ [43]. The parameter q is proportional to the square of the pre-tilting electric field [30–32, 43, 45]. The defocusing nematic equations then consist of an NLS-type equation (1) for the electric field of the light beam and an elliptic equation (2) for the nematic response. While these equations have been introduced in the context of the nonlinear optics of nematic liquid crystals, they apply to a diverse range of optical applications. They also apply to optical beam propagation in nonlinear thermal media [34, 37, 46], such as lead glasses [47–49], and certain photorefractive crystals [50]. In general, a system of equations similar to the nematic equations applies to optical beam propagation in any medium for which the nonlinear response is accompanied by some diffusive mechanism [51]. In addition, equations similar to (1) and (2) arise in certain models of fluid turbulence [52, 53] and in quantum gravity as the Schrödinger-Newton equations [54].

Since the electric field equation (1) is a defocusing NLS-type equation, it possesses undular bore, or dispersive shock wave, solutions [42]. The simplest initial condition which will generate an undular bore is a discontinuous jump in the electric field intensity between two values, as for the classic undular bore solution of the KdV equation [8, 9],

$$u(x, 0) = \begin{cases} u_3, & x < 0 \\ u_1, & x > 0 \end{cases}, \quad (3)$$

where $u_3 > u_1 \geq 0$. The director equation (2) shows that the consistent initial condition

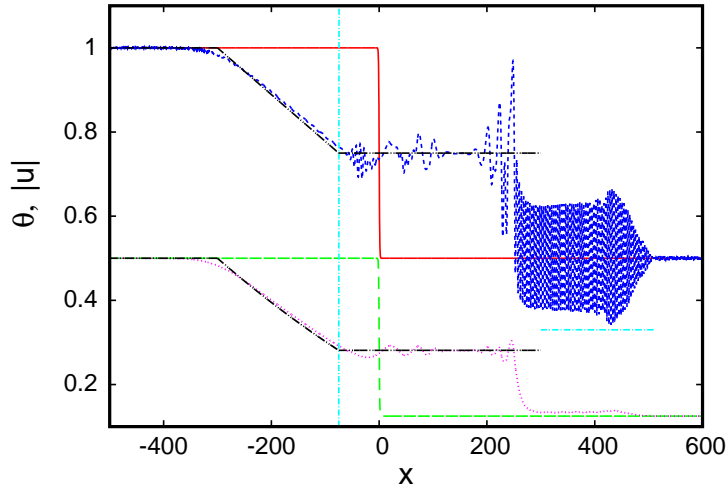


Figure 1: (Color online) Comparison between numerical solution of dark nematicon equations (1) and (2) and theoretical solution for initial jump condition (3). The lower curves are θ and the upper curves are $|u|$. Initial condition for $|u|$: red (solid) line; initial condition for θ : green (long dash) line; numerical solution for $|u|$ at $z = 300$: blue (short dashed) line; numerical solution for θ at $z = 300$: pink (dotted) line; theoretical solution: black (dot-dot-dash) line. KdV bore and uniform wavetrain limits: light blue (dot-dash) line. The parameter values are $u_3 = 1.0$, $u_1 = 0.5$, $\nu = 200$ and $q = 2$.

for the director is

$$\theta(x, 0) = \begin{cases} \frac{u_3^2}{q}, & x < 0 \\ \frac{u_1^2}{q}, & x > 0 \end{cases}. \quad (4)$$

3. Undular bore theory

A typical numerical solution of the nematic equations (1) and (2) for the initial condition (3) for an experimental value of ν is shown in Figure 1. It can be seen that the two initial levels are linked by a backward expanding expansion wave to the level u_3 , a flat shelf with a modulated wavetrain on it which resembles a KdV bore and, lastly, a nearly uniform wavetrain bringing the solution back to $u = u_1$. Except for the wavetrain region, the spatial derivatives of u and θ are small and so the solution is non-dispersive in these regions. This structure is similar to that for the defocusing NLS undular bore [42]. Indeed, the nematic equations (1) and (2) reduce to the defocusing NLS equation in the limit $\nu \rightarrow 0$. However, experimental values of ν are large, $O(100)$ [43]. While outside the wavetrain region the derivatives of u and θ are small, it should be noted that the derivative θ_{xx} in the director equation (2) is multiplied by the large quantity ν , which could mean that $\nu\theta_{xx}$ is $O(1)$. This is not the case for large z as it will be shown below that, apart from the wavetrain region, $\theta_{xx} = O(z^{-2})$ for large z , so the neglect of $\nu\theta_{xx}$ outside the dispersive wave region is valid in this limit. The structure of the undular bore is very different in the limits $\nu \rightarrow 0$ and ν large, as can be seen on comparing the solution for $\nu = 200$ shown in Figure 1 with the solution for $\nu = 0.1$ shown in Figure 2. The solutions for the two values of ν are similar away from the bore, which will be

taken up below. However, the bore for large ν has a lead wavetrain consisting of waves of nearly equal amplitude with a small front which brings the solution down to the initial level u_1 , together with bright waves on the shelf linking the levels ahead and behind the bore. The solution in the non-dispersive regions are easiest to determine and will be taken up first.

The structure of the bore in the local (ν small) and nonlocal (ν large) regimes is then distinct, with a key difference being the KdV-type bore wavetrain on the intermediate shelf. Previous experimental work on two dimensional radially symmetric undular bores in thermal nonlinear optical media [34] shows evidence of this KdV-type bore, see Figure 5 of this work, as do numerical solutions of the governing equations, which are the same as the nematic equations (1) and (2), for an $O(1)$ nonlocality parameter [34], see Figure 4 of this work. Furthermore, other numerical solutions of the equations governing optical beam propagation in a thermal nonlinear medium [36] show structures similar to the undular bore solution of Figure 1 for an $O(1)$ nonlocality, see Figure 11 of this work. These numerical solutions show a KdV-type bore preceded by a nearly uniform wavetrain. However, the solutions were generated from a finite initial condition via a gradient catastrophe. Such finite initial conditions will not generate true undular bores, but only approximations to such for low values of z , due to the finite initial condition being unable to continually generate waves as the bore spreads, as is possible for the initial step (3) due to it being non-zero as $x \rightarrow -\infty$.

To determine the solution in these non-dispersive regions the Madelung transformation [42]

$$u = \sqrt{\rho}e^{i\phi}, \quad v = \phi_x \quad (5)$$

is used to separate the dispersive and non-dispersive portions of the electric field equation (1). Using this transformation, the nematic equations (1) and (2) become

$$\frac{\partial \rho}{\partial z} + \frac{\partial}{\partial x}(\rho v) = 0, \quad (6)$$

$$\frac{\partial v}{\partial z} + v \frac{\partial v}{\partial x} + 2 \frac{\partial \theta}{\partial x} - \frac{\partial}{\partial x} \left(\frac{\rho_{xx}}{4\rho} - \frac{\rho_x^2}{8\rho^2} \right) = 0, \quad (7)$$

$$\nu \frac{\partial^2 \theta}{\partial x^2} - 2q\theta = -2\rho, \quad (8)$$

which is termed the hydrodynamic form of the nematic equations [11, 42] due to the similarity of these equations with those for shallow water waves and compressible gas dynamics [1].

It can be seen from Figure 1 that away from the bore, the derivative of θ is small, as discussed above. Hence, away from the bore, the solution of the nematic equations (1) and (2) for the initial condition (3) is governed by the hyperbolic dispersionless equations

$$\frac{\partial \rho}{\partial z} + \frac{\partial}{\partial x}(\rho v) = 0, \quad (9)$$

$$\frac{\partial v}{\partial z} + v \frac{\partial v}{\partial x} + 2 \frac{\partial \theta}{\partial x} = 0, \quad (10)$$

$$\theta = \frac{\rho}{q}. \quad (11)$$

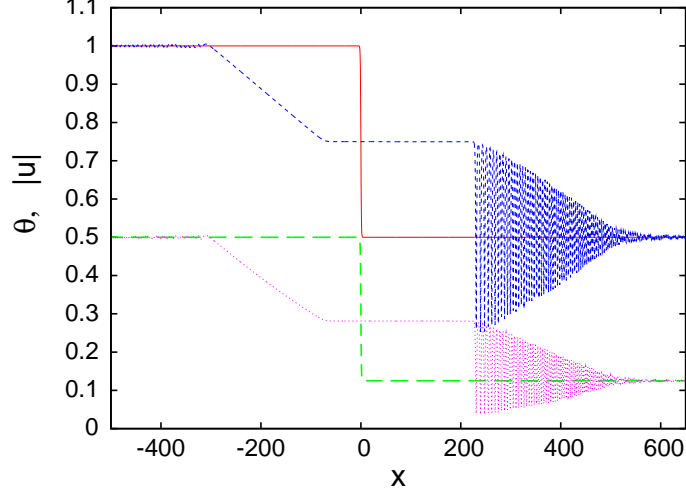


Figure 2: (Color online) Numerical solution of dark nematicon equations (1) and (2) for initial jump condition (3). The lower curve is θ and the upper curve is $|u|$. Initial condition for $|u|$: red (solid) line; initial condition for θ : green (long dash) line; numerical solution for $|u|$ at $z = 300$: blue (short dash) line; numerical solution for θ at $z = 300$: pink (dotted) line. The parameter values are $u_3 = 1.0$, $u_1 = 0.5$, $\nu = 0.1$ and $q = 2$.

In Riemann invariant form, these equations are

$$v + \frac{2\sqrt{2}}{\sqrt{q}}\sqrt{\rho} = \text{constant} \quad \text{on} \quad C_+ : \frac{dx}{dz} = V_+ = v + \frac{\sqrt{2}}{\sqrt{q}}\sqrt{\rho} \quad (12)$$

$$v - \frac{2\sqrt{2}}{\sqrt{q}}\sqrt{\rho} = \text{constant} \quad \text{on} \quad C_- : \frac{dx}{dz} = V_- = v - \frac{\sqrt{2}}{\sqrt{q}}\sqrt{\rho}, \quad (13)$$

with θ given by (11). These dispersionless equations applying outside the bore region are a scaled version of those for the standard NLS equation [27, 42]. Hence, the solution of the nematic equations (1) and (2) outside the bore region will be the same as that for the NLS equation outside the undular bore region.

The simplest solution of the dispersionless equations corresponds to the dam break problem of shallow water wave theory [1], for which $u_1 = 0$. The Riemann invariant form (12) and (13) gives the simple wave solution

$$|u| = \sqrt{\rho} = \begin{cases} u_3, & \frac{x}{z} < -\frac{\sqrt{2}u_3}{\sqrt{q}} \\ \frac{\sqrt{q}}{3\sqrt{2}} \left(\frac{2\sqrt{2}u_3}{\sqrt{q}} - \frac{x}{z} \right), & -\frac{\sqrt{2}u_3}{\sqrt{q}} \leq \frac{x}{z} \leq \frac{2\sqrt{2}u_3}{\sqrt{q}} \\ 0, & \frac{2\sqrt{2}u_3}{\sqrt{q}} < \frac{x}{z}. \end{cases} \quad (14)$$

and

$$v = \begin{cases} 0, & \frac{x}{z} < -\frac{\sqrt{2}u_3}{\sqrt{q}} \\ \frac{2\sqrt{2}u_3}{3\sqrt{q}} + \frac{2x}{3z}, & -\frac{\sqrt{2}u_3}{\sqrt{q}} \leq \frac{x}{z} \leq \frac{2\sqrt{2}u_3}{\sqrt{q}} \\ \frac{2\sqrt{2}u_3}{\sqrt{q}}, & \frac{2\sqrt{2}u_3}{\sqrt{q}} < \frac{x}{z} \end{cases} \quad (15)$$

generated on the C_- characteristics for this case. The solution of the nematic equations (1) and (2) for the initial condition (3) is now complete for this simple dam break case since, as for the defocusing NLS equation [42], no undular bore is generated, corresponding to no shock (hydraulic jump) being generated for the dam break problem [1], as well as no uniform wavetrain of the form seen in Figure 1 being generated. This solution will be compared with full numerical solutions of the nematic equations (1) and (2) in the next section.

When the level ahead u_1 is non-zero, then as well as the simple wave on the characteristics C_- , there is an upstream propagating undular bore and an upstream propagating uniform wavetrain if the jump height is large enough. The simple wave is separated from the upstream level by a shelf of height $u_2 = \sqrt{\rho_2}$, so that $u = u_2 e^{iv_2 x}$ on the shelf. The Riemann invariant form (12) and (13) gives the simple wave solution

$$|u| = \sqrt{\rho} = \begin{cases} u_3, & \frac{x}{z} < -\frac{\sqrt{2}u_3}{\sqrt{q}} \\ \frac{\sqrt{q}}{3\sqrt{2}} \left[\frac{2\sqrt{2}u_3}{\sqrt{q}} - \frac{x}{z} \right], & -\frac{\sqrt{2}u_3}{\sqrt{q}} \leq \frac{x}{z} \leq \frac{\sqrt{2}}{\sqrt{q}} (2u_3 - 3\sqrt{\rho_2}) \\ \sqrt{\rho_2}, & \frac{\sqrt{2}}{\sqrt{q}} (2u_3 - 3\sqrt{\rho_2}) < \frac{x}{z} \leq v_- \end{cases} \quad (16)$$

and

$$v = \begin{cases} 0, & \frac{x}{z} < -\frac{\sqrt{2}u_3}{\sqrt{q}} \\ \frac{2\sqrt{2}u_3}{3\sqrt{q}} + \frac{2x}{3z}, & -\frac{\sqrt{2}u_3}{\sqrt{q}} \leq \frac{x}{z} \leq \frac{\sqrt{2}}{\sqrt{q}} (2u_3 - 3\sqrt{\rho_2}) \\ \frac{2\sqrt{2}}{\sqrt{q}} (u_3 - \sqrt{\rho_2}), & \frac{\sqrt{2}}{\sqrt{q}} (2u_3 - 3\sqrt{\rho_2}) < \frac{x}{z} \leq v_- \end{cases} \quad (17)$$

generated along the C_- characteristics. It is then clear that

$$v_2 = \frac{2\sqrt{2}}{\sqrt{q}} (u_3 - \sqrt{\rho_2}). \quad (18)$$

The speed v_- is the speed of the trailing edge of the uniform wavetrain, as seen in Figure 1. Both this speed and the shelf height u_2 are yet to be determined. The height $u_2 = \sqrt{\rho_2}$ is determined by the requirement that the Riemann invariant along the characteristic C_- is conserved through the bore [11, 12, 27]. Hence

$$v_2 - \frac{2\sqrt{2}}{\sqrt{q}} \sqrt{\rho_2} = -\frac{2\sqrt{2}}{\sqrt{q}} \sqrt{\rho_1} = -\frac{2\sqrt{2}}{\sqrt{q}} u_1, \quad (19)$$

which on using expression (18) gives

$$u_2 = \sqrt{\rho_2} = \frac{u_3 + u_1}{2}. \quad (20)$$

This result is clear from the underlying directional symmetry. It was shown by El [11, 12] that the Riemann invariant on the characteristic C_- is conserved through the NLS bore structure consisting of a (dark) bore linking two levels. It can be seen from Figures 1 and 2 that the wave structure for the nematic bore is more complicated than the simple NLS structure. It will be shown in Section 4 that there is a KdV bore on the intermediate level u_2 , which is preceded by a linear wavetrain, which is clear from Figure 1. The conservation of the Riemann invariant on the characteristic C_- across this combined structure

then does not directly follow from the results of El [11, 12]. However, this Riemann invariant is conserved as the wavetrain preceding the bore, to a first approximation, is linear and so does not affect the modulations. The calculation of the next, nonlinear, correction to the intermediate level u_2 is then non-trivial as the Riemann invariant argument of El does not hold. This is an open question which deserves further investigation. The gradient v of the phase ϕ of the wavetrain on the shelf is then, from (18),

$$v_2 = \frac{\sqrt{2}}{\sqrt{q}} (u_3 - u_1). \quad (21)$$

The velocity v_- of the leading edge of the intermediate level u_2 will be determined in the next section.

The final parts of the solution for the initial condition (3) to determine are the wavetrain preceding the intermediate mean level u_2 and the wavetrain on the level u_2 , as seen in Figure 1. This presents more difficulties than for the regions away from these wavetrains. Undular bore solutions are found as simple wave solutions of the modulation equations for the underlying governing equation. These simple wave solutions are easily found when the modulation equations can be set in Riemann invariant form. If the underlying equation is integrable with an inverse scattering solution, there is a standard method to obtain this Riemann invariant form [10]. If there is no inverse scattering solution, then finding the Riemann invariant form of any modulation equations is a non-trivial task. In these situations, El [11, 12] developed a method by which the details of the leading and trailing waves of the bore can be determined, but not the interior details of the bore. This method will now be applied to try to determine the leading and trailing edges of a bore linking the non-dispersive regions, as seen in Figure 1.

The work of El [11, 12, 25] shows that the leading edge of a bore is determined from the (linear) dispersion relation for the governing equation. Linearising the nematicon equations (6)–(8) about the background mean levels $\bar{\rho}$ and \bar{v} with

$$\rho = \bar{\rho} + \tilde{\rho}, \quad v = \bar{v} + \tilde{v}, \quad \theta = \frac{\bar{\rho}}{q} + \tilde{\theta}, \quad (22)$$

where $|\tilde{\rho}| \ll \bar{\rho}$, $|\tilde{v}| \ll |\bar{v}|$ and $|\tilde{\theta}| \ll \bar{\rho}/q$, gives the linearised nematicon equations

$$\frac{\partial \tilde{\rho}}{\partial z} + \bar{\rho} \frac{\partial \tilde{v}}{\partial x} + \bar{v} \frac{\partial \tilde{\rho}}{\partial x} = 0, \quad (23)$$

$$\frac{\partial \tilde{v}}{\partial z} + \bar{v} \frac{\partial \tilde{v}}{\partial x} + 2 \frac{\partial \tilde{\theta}}{\partial x} - \frac{1}{4\bar{\rho}} \frac{\partial^3 \tilde{\rho}}{\partial x^3} = 0, \quad (24)$$

$$\nu \frac{\partial^2 \tilde{\theta}}{\partial x^2} - 2q\tilde{\theta} = -2\tilde{\rho}. \quad (25)$$

The dispersion relation for right propagating waves for these linearised equations is

$$\omega = k\bar{v} + \frac{\sqrt{\bar{\rho}k}}{\sqrt{\nu k^2 + 2q}} \left[\frac{\nu k^2 + 2q}{4\bar{\rho}} k^3 + 4k \right]^{1/2}. \quad (26)$$

In the present work we shall be interested in the experimental regime for which ν is large [43]. For large ν , the dispersion relation (26) is

$$\omega = k\bar{v} + \frac{1}{2}k^2 + \frac{4\bar{\rho}}{9\nu k^2} + O(\nu^{-2}). \quad (27)$$

In the opposite limit $\nu \rightarrow 0$ for which the nematonic equations (1) and (2) become the defocusing NLS equation, the dispersion relation is

$$\omega = k\bar{v} + k^2 \sqrt{\frac{1}{4}k^2 + \frac{2}{q}\bar{\rho}} - \frac{\nu\bar{\rho}k^3}{2q^2} \left[\frac{1}{4}k^2 + \frac{2}{q}\bar{\rho} \right]^{-1/2} + O(\nu^2), \quad (28)$$

which is the same to first order as that for the defocusing NLS equation [12, 25], as required.

Let us now use the method of El [11, 12] to try to determine the leading, linear wave edge of a bore linking the level u_2 to the level u_1 . This method finds the mean values of ρ and v , $\bar{\rho}$ and \bar{v} , respectively, at the leading and trailing edges of the bore. It is these mean values which are given by Whitham modulation theory [1]. Let us take the dispersion relation (27) to first order in ν^{-1} . The mean phase gradient \bar{v} in this dispersion relation needs to be determined. It was shown by El [11, 12] that the Riemann invariant on C_- (13) is conserved through the bore. Hence, we have

$$\bar{v} = 2\sqrt{\frac{2}{q}}(\sqrt{\bar{\rho}} - u_1) \quad (29)$$

on linking to the initial state $\bar{\rho} = u_1^2$ and $\bar{v} = 0$ ahead of the bore. We then have that the wavenumber k at the leading edge of the bore is determined by the differential equation [11, 12, 25]

$$\frac{dk}{d\bar{\rho}} = \frac{\frac{\partial\omega}{\partial\bar{\rho}}}{V_+(\bar{\rho}, \bar{v}) - \frac{\partial\omega}{\partial k}} = \frac{k}{\bar{\rho} - k\sqrt{q\bar{\rho}/2}} \quad (30)$$

to leading order in ν^{-1} , with the boundary condition $k(u_2) = 0$ to link the leading edge of the bore with the trailing, (dark) solitary wave edge. The velocity $V_+(\bar{\rho}, \bar{v})$ is the characteristic velocity (12) evaluated at the mean height $\bar{\rho}$ and mean phase gradient \bar{v} . The solution of this differential equation is

$$k = C\bar{\rho} \left(1 + \sqrt{\frac{q}{2}} \frac{k}{\sqrt{\bar{\rho}}} \right)^2, \quad (31)$$

where C is a constant of integration. The boundary condition $k(\rho_2) = 0$, where $\rho_2 = u_2^2$, gives $k \equiv 0$. This result shows that there can be no undular bore linking the level u_2 to the level u_1 in the physical limit of ν large. This conclusion is consistent with the numerical solutions for large ν and small ν shown in Figures 1 and 2. The non-existence of a bore solution is due to there being no $\bar{\rho}$ term in the dispersion relation (27) at first order in ν^{-1} , so that the dispersion relation does not support a change in mean level that is the basis of a bore. Including higher order terms in $1/\nu$ in the dispersion relation (27) will not yield a valid bore solution as these higher order terms cannot result in an $O(1)$ change in k (and $\bar{\rho}$) through a bore.

The nature of the wavetrain preceding the intermediate level u_2 will be taken up in the next section. It is linked to the KdV-type bore wavetrain seen on the level u_2 in Figure 1. The solution for this wavetrain needs to be found before the wavetrain ahead of the intermediate level u_2 can be determined.

4. Korteweg-de Vries limit

The numerical solution displayed in Figure 1 shows that there is a wavetrain on the intermediate level u_2 given by (20) which closely resembles a KdV bore [8, 9]. The reason for this wavetrain and its relation to the KdV bore will now be discussed.

It has been shown that in the limit of small amplitude long waves on a background carrier wave, the defocusing NLS equation reduces to the KdV equation with the KdV solitons waves of depression [55, 56]. Recent work has further shown that the nematic equations (1) and (2) also reduce to the KdV equation in this limit [57]. If the background carrier wave has amplitude u_0 , then the appropriate asymptotic expansions for small amplitude waves about this carrier wave are

$$u = [u_0 + \epsilon^2 a_1(\xi, \eta) + \epsilon^4 a_2(\xi, \eta) + \dots] e^{-2iu_0^2 z/q + i\phi(\xi, \eta)}, \quad (32)$$

$$\phi = \epsilon \phi_1(\xi, \eta) + \epsilon^3 \phi_2(\xi, \eta) + \epsilon^5 \phi_3(\xi, \eta) + \dots, \quad (33)$$

$$\theta = \frac{u_0^2}{q} + \epsilon^2 \theta_1(\xi, \eta) + \epsilon^4 \theta_2(\xi, \eta) + \epsilon^6 \theta_3(\xi, \eta) + \dots, \quad (34)$$

where $0 < \epsilon \ll 1$ and

$$\xi = \epsilon(x - Uz), \quad \eta = \epsilon^3 z. \quad (35)$$

The stretched variables ξ and η are the usual variables used to obtain the KdV equation in standard form [1]. Substituting these expansions into the nematic equations (1) and (2), we obtain at $O(\epsilon^2)$ and $O(\epsilon^3)$

$$\frac{\partial \phi_1}{\partial \xi} = \frac{4u_0}{qU} a_1 \quad \text{and} \quad U^2 = \frac{2u_0^2}{q}. \quad (36)$$

At $O(\epsilon^4)$ and $O(\epsilon^5)$ two partial differential equations involving a_2 and ϕ_2 are obtained. These equations are the same if a compatibility condition is satisfied, which is the KdV equation

$$\frac{\partial a_1}{\partial \eta} + \frac{6u_0}{qU} a_1 \frac{\partial a_1}{\partial \xi} + \left(\frac{\nu U}{4q} - \frac{qU}{16u_0^2} \right) \frac{\partial^3 a_1}{\partial \xi^3} = 0. \quad (37)$$

In the NLS limit ν small of the nematic equations (1) and (2), soliton solutions of this KdV equation are waves of depression, dark solitons, in agreement with the NLS asymptotic analysis [55, 56]. As previously stated, for the usual experimental operating regime for nonlinear optical beam propagation in nematic liquid crystals ν is large, $\nu = O(100)$ [43], which is the regime considered in the present work. In this regime, KdV soliton solutions of (37) are then waves of elevation, bright solitons. The KdV equation (37) can be set in standard form

$$\frac{\partial a_1}{\partial T} + 6a_1 \frac{\partial a_1}{\partial X} + \frac{\partial^3 a_1}{\partial X^3} = 0 \quad (38)$$

via the coordinate transformations

$$\xi = (2q)^{1/4} \left[\frac{\nu U}{4q} - \frac{qU}{16u_0^2} \right]^{1/2} X, \quad \eta = (2q)^{3/4} \left[\frac{\nu U}{4q} - \frac{qU}{16u_0^2} \right]^{1/2} T. \quad (39)$$

Note that it has been assumed that the nematic cell is in the highly nonlocal regime with ν large, so that these coordinate transformations are physical. For the present work, the level $u_0 = u_1$, as is clear from Figure 1.

The KdV equation has a standard bore solution [8, 9] obtained as a centred simple wave solution of the modulation equations for the KdV equation [1, 5]. This solution shows that the KdV bore consists of solitons of amplitude 2Δ at its leading edge, where Δ is the height of the initial jump generating the bore, and linear waves at its trailing edge. Identifying $\Delta = u_2 - u_1 = (u_3 - u_1)/2$, we have that the total height of the lead wave of the KdV bore on the intermediate level is

$$a_s = u_3 \quad (40)$$

as it rises from the background level u_1 . In the (X, T) coordinates the KdV bore occupies the region $-6(u_2 - u_1) \leq X/T \leq 4(u_2 - u_1)$ [8, 9]. Transforming back to the physical coordinates (x, z) using the scalings (39) which set the KdV equation in standard form, the asymptotic coordinates given by (35) and noting that ξ and X are coordinates moving with the velocity $U = \sqrt{2}u_0/\sqrt{q} = \sqrt{2}u_1/\sqrt{q}$, we have that the KdV bore on the shelf u_2 occupies the region

$$\sqrt{\frac{2}{q}} \left(\frac{5}{2}u_1 - \frac{3}{2}u_3 \right) \leq \frac{x}{z} \leq \sqrt{\frac{2}{q}} u_3. \quad (41)$$

It is then clear that the leading edge of the intermediate shelf has the velocity

$$v_- = \sqrt{\frac{2}{q}} u_3. \quad (42)$$

Now that the bore on the intermediate level u_2 has been determined, the wavetrain preceding it and bringing the solution down to u_1 can be further considered.

As previously noted, the numerical solution for $\nu = 200$ displayed in Figure 1, on comparison with the standard bore solution for $\nu = 0.1$ displayed in Figure 2, shows that the mean level u_2 is not preceded by a bore, but a wavetrain of constant amplitude preceded by a short front taking it down to the original level u_1 . This wavetrain is generated by a phase mismatch between the phase of the soliton at the leading edge of the KdV bore and the phase $v = 0$ of the initial level ahead. The phase (36) for the KdV expansion gives that

$$\bar{v} = 4\sqrt{\frac{2}{q}}(u_3 - u_1) = 4v_2 \quad (43)$$

at the leading edge of the KdV bore. A wavetrain must then bring this phase down to $\bar{v} = 0$, which is the initial state ahead. The position of the leading and trailing edges of this uniform wavetrain can be found by a simple group and phase velocity argument, as for the classical Kelvin ship wave problem [1]. The numerical solution displayed in Figure 1 shows that the director under the uniform wavetrain is essentially constant at

$$\theta = \Theta_1 = \frac{u_1^2}{q}. \quad (44)$$

The director is uniform in the region of the wavetrain due to the nonlocal response of the director [45] to the rapid oscillation of $|u|$ of the wavetrain. This nonlocality smooths

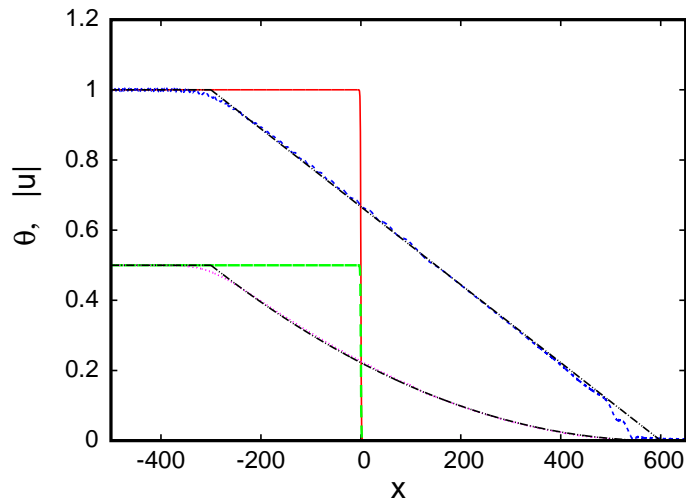


Figure 3: (Color online) Comparison between numerical solution of dark nematicon equations (1) and (2) and theoretical solution for initial jump condition (3). The lower curves are θ and the upper curves are $|u|$. Initial condition for $|u|$: red (solid) line; initial condition for θ : green (dot-dash) line; numerical solution for $|u|$ at $z = 300$: blue (dash) line; numerical solution for θ at $z = 300$: pink (dotted) line; theoretical solution: black (dot-dot-dash) line. The parameters are $u_3 = 1.0$, $u_1 = 0.0$, $\nu = 200$ and $q = 2$.

out the response of the director to the electric field, resulting in the director essentially reacting to the mean of the rapid oscillation of $|u|$, as has been noted previously in studies of bores in nematic liquid crystals [40, 58]. Hence, the electric field equation (1) in the region of the uniform wavetrain can be approximated by

$$i \frac{\partial u}{\partial z} + \frac{1}{2} \frac{\partial^2 u}{\partial x^2} - 2\Theta_1 u = 0, \quad (45)$$

for which the dispersion relation for right propagating waves on a background $u_1 \exp(-2i\Theta_1 z)$ is

$$\omega = \frac{1}{2} k^2 + 2\Theta_1. \quad (46)$$

This restricted dispersion relation differs from the full dispersion relation (26) due to the neglect of a linear wavetrain in the director θ . The phase c and group c_g velocities for the dispersion relation (46) are

$$c = \frac{1}{2} k + \frac{2\Theta_1}{k} \quad \text{and} \quad c_g = k. \quad (47)$$

The extent of the uniform wavetrain preceding the KdV bore can be determined from the phase and group velocities (47). The wavetrain has the same phase velocity as the velocity of the lead solitary wave of the KdV bore behind it, so that

$$\frac{1}{2} k + \frac{2\Theta_1}{k} = \sqrt{\frac{2}{q}} u_3. \quad (48)$$

Noting that $\Theta_1 = u_1^2/q$, we have that

$$k = \sqrt{\frac{2}{q}} \left[u_3 + \sqrt{u_3^2 - 2u_1^2} \right] \quad (49)$$

on taking the positive square root to give a sensible result for the group velocity as $u_1 \rightarrow 0$. The group velocity of this wavetrain, which gives the position of the front of the wavetrain, is then

$$c_g = k = \sqrt{\frac{2}{q}} \left[u_3 + \sqrt{u_3^2 - 2u_1^2} \right]. \quad (50)$$

It can be seen that this uniform wavetrain can only exist if $u_1 < u_3/\sqrt{2}$. For $u_1 > u_3/\sqrt{2}$ the wavetrain ahead of the KdV bore will be evanescent [1].

The analytical results of this section will be compared with full numerical solutions of the nematic equations (1) and (2) in the next section.

5. Comparison with numerical solutions

For the comparisons of the analytical results of the previous sections with numerical solutions, the electric field equation (1) was solved numerically using a pseudo-spectral method based on that of Fornberg and Whitham [9], which was originally used to find the undular bore solution of the KdV equation. The pseudo-spectral method used here differs from that of Fornberg and Whitham in that the electric field equation (1) is advanced in z in Fourier space using a fourth order Runge-Kutta scheme, rather than in real space using a leap frog scheme as in Fornberg and Whitham. Full details of this modified pseudo-spectral scheme can be found in [59]. The elliptic director equation (2) was solved numerically using a Fourier method whose details are given in [60]. The director equation (2) has a large coefficient ν in front of the second derivative θ_{xx} , so that it would appear to be a stiff equation numerically. This is not the case, however, as there are no boundary layers at the ends of the computational domain due to the exponential decay of the solution for θ to the value at the numerical boundaries where the boundary condition $\theta = 0$ was imposed.

The simplest solution of the nematic equations (1) and (2) for the initial condition (3) is with the level ahead 0, $u_1 = 0$, the dam break problem. The solution for this case is shown in Figure 3. It can be seen, as predicted, that the solution consists solely of expansion waves in the electric field u and the director θ , as for the defocusing NLS equation [42]. The modulation theory solution in this case is (14) and (15). It can be seen that there is near perfect agreement between the numerical and modulation solutions for both the electric field and the director. There is slight disagreement where the expansion waves join the initial levels ahead and behind. This is due to the discontinuity in the derivatives being smoothed by dispersion [9].

Figure 1 shows the solution for a typical case for which $u_1 \neq 0$. As mentioned above, the solution for the electric field u shows many similarities with the NLS bore, as shown in Figure 2. The expansion waves are similar, but the bore structure is entirely different. As noted in Section 4 there is a KdV bore on the intermediate level u_2 which is preceded by a uniform wavetrain which brings the solution down to the level u_1 , this wavetrain being determined by a phase and group velocity argument, resulting in its leading edge

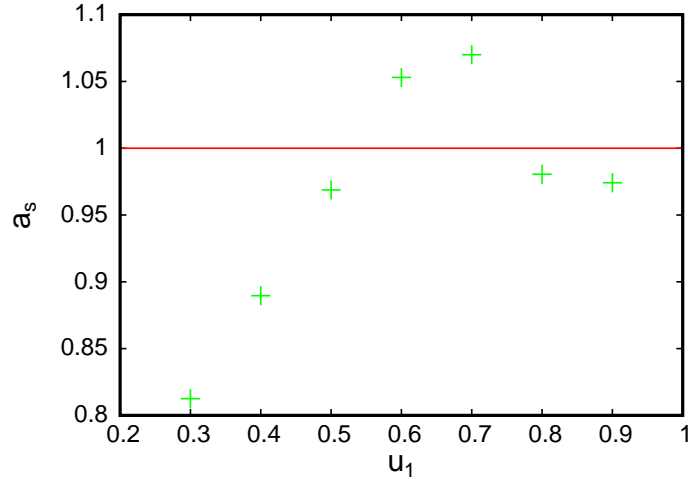


Figure 4: (Color online) Comparison of the height of the lead soliton of the KdV bore as given by the numerical solution of the dark nematic equations (1) and (2) and the theoretical solution (40). Numerical solution: (green) crosses; theoretical solution: (red) line. The parameter values are $u_3 = 1.0$, $\nu = 200$ and $q = 2$.

being given by (50) and its trailing edge by (42). It can be seen from this figure that the expansion wave solution (16) with $\theta = |u|^2/q$ is in excellent agreement with the numerical solution in the region between the levels u_3 and u_2 , as for the dam break case of Figure 3. Again, there is some disagreement where this expansion wave joins to u_3 and u_2 . This is due to the discontinuities in derivative at the edges being smoothed out by dispersion, resulting in the generation of dispersive wavetrains [9]. The height of the lead soliton on the intermediate shelf u_2 is $a_s = 0.9688$, which is in excellent agreement with the theoretical value (40), $a_s = 1.0$. The waves in the KdV bore have a large wavelength. This is due to the large nonlocality ν , as can be seen from the spatial scaling in (39). Also shown in Figure 1 is a horizontal light blue (dot-dash) line giving the extent of the uniform wavetrain and located under this wavetrain, the trailing edge being given by (42) and the leading edge by (50). Again, there is excellent agreement for the extent of this wavetrain as given by the phase and group velocity argument of the previous section. The final comparison shown in Figure 1 is for the trailing edge of the KdV bore as given by (41). The position of this trailing edge is shown by the vertical light blue (dot-dash) line. The agreement between the numerical and analytical solutions is less clear for this trailing edge position due to the interaction between the KdV bore and the expansion wave linking the initial level u_3 and the intermediate level u_2 .

Figure 4 shows a comparison between the height of the lead soliton of the KdV bore on the intermediate shelf u_2 as given by the numerical solution of the nematic equations (1) and (2) and the KdV bore solution (40). The analytical and numerical amplitudes are in excellent agreement for $u_1 \geq 0.5$, with the agreement decreasing as the initial jump height increases. This increasing disagreement is expected as the KdV equation (37) was derived in the limit of small deviations from a background level, which is equivalent to small initial jumps.

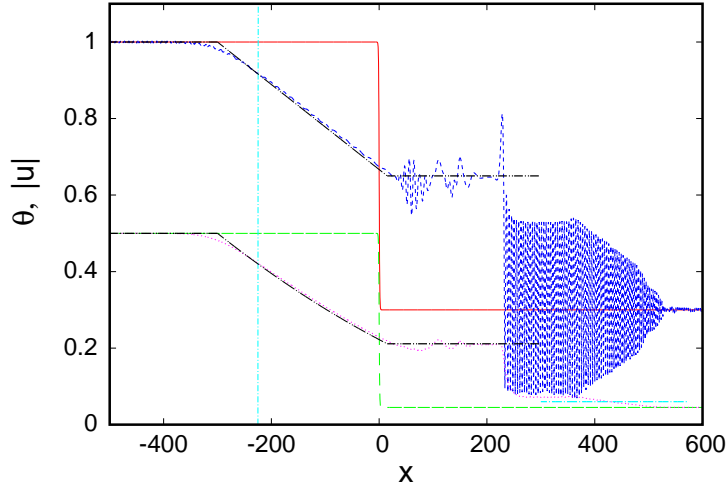


Figure 5: (Color online) Comparison between numerical solution of dark nematicon equations (1) and (2) and theoretical solution for initial jump condition (3). The lower curves are θ and the upper curves are $|u|$. Initial condition for $|u|$: red (solid) line; initial condition for θ : green (long dash) line; numerical solution for $|u|$ at $z = 300$: blue (short dash) line; numerical solution for θ at $z = 300$: pink (dotted) line; theoretical solution: black (dot-dot-dash) line. KdV bore and uniform wavetrain limits: light blue (dot-dash) line. The parameter values are $u_3 = 1.0$, $u_1 = 0.3$, $\nu = 200$ and $q = 2$.

Figure 5 shows a similar comparison between the analytical and numerical solutions as Figure 1, but for $u_1 = 0.3$. For this value of u_1 the solution is near the vacuum point [42] at which the lead wavetrain reaches $u = 0$. There is, again, excellent agreement between the numerical and modulation solutions for the expansion wave portions of the solution. However, as noted from Figure 4, there is not good agreement for the amplitude of the lead soliton of the KdV bore on the intermediate level u_2 and the position of the trailing edge of the KdV bore as given by (41). As noted previously, this is due to the KdV equation (37) being derived in the limit of small deviations from a background level, which is not the case for this Figure as the jump height is 0.7. Similarly, the leading and trailing edges of the lead uniform wavetrain as given by (50) and (42) are in reasonable agreement with the numerical solution, but the agreement is not as good as for the lower jump height of Figure 1. Finally, as seen from the height comparison of Figure 4, the height of the lead soliton of the KdV bore, given by (40) as $a_s = 1$, is not in good agreement with the numerical solution. This is again due to the jump height $u_2 - u_1$ not being small as assumed in the derivation of the KdV equation (37).

The phase and group velocity argument of Section 4, resulting in the wavenumber (49) and group velocity (50) of the uniform wavetrain, gave that the uniform wavetrain ahead of the KdV bore ceases to exist for $u_1 > u_3/\sqrt{2}$. Numerical solutions showed that the leading uniform wavetrain ceases to exist for $u_1 > 0.69$ for $u_3 = 1.0$, which is in excellent agreement with the analytical prediction. Figure 6 shows a comparison for a case just below the analytical cut-off point, $u_1 = 1/\sqrt{2}$ for $u_3 = 1$. The solution shown in Figure 6 is just above the numerical cut-off $u_1 = 0.69$ and there is a small wavetrain ahead of the KdV bore. While the solution in this figure is just below the analytical cut-

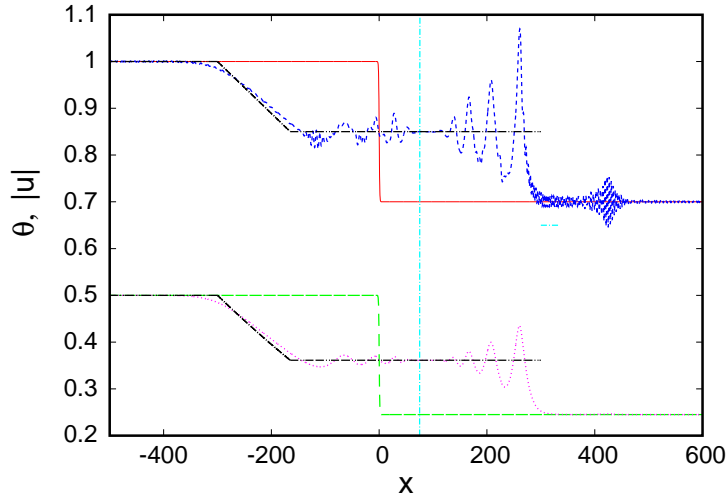


Figure 6: (Color online) Comparison between numerical solution of dark nematicon equations (1) and (2) and theoretical solution for initial jump condition (3). The lower curves are θ and the upper curves are $|u|$. Initial condition for $|u|$: red (solid) line; initial condition for θ : green (long dash) line; numerical solution for $|u|$ at $z = 300$: blue (short dash) line; numerical solution for θ at $z = 300$: pink (dotted) line; theoretical solution: black (dot-dot-dash) line. KdV bore and uniform wavetrain limits: light blue (dot-dash) line. The parameter values are $u_3 = 1.0$, $u_1 = 0.7$, $\nu = 200$ and $q = 2$.

off, the light blue (dot-dash) line giving the limits of the wavetrain as predicted by (42) and (50) shows that the theory predicts that the wavetrain is practically non-existent. The trailing edge of the KdV bore as given by (41) and shown by the vertical light blue (dot-dash) line is in good agreement with the numerical solution. As for the comparisons of the previous figures, the expansion wave portion (16) of the analytical solution is in good agreement with the numerical solution. Finally, as seen in the height comparison of Figure 4, the height of the lead soliton of the KdV bore is in good agreement with the analytical value $a_s = 1$.

6. Conclusions

The undular bore solution of the equations governing nonlinear optical beam propagation in a defocusing nematic liquid crystal has been derived. These equations form a coupled system of an NLS-type equation for the electric field of the light beam propagating in the nematic medium and an elliptic equation for the response of the nematic molecules to this light. While the electric field equation is of NLS-type, it is found that the undular bore generated by an initial discontinuity in the intensity of the electric field is of KdV-type, consisting of bright waves rather than the dark waves of an NLS bore, in the usual experimental regime of a highly nonlocal response, that is ν large. Ahead of this KdV bore is a uniform wavetrain with a front which brings this wavetrain down to the initial state ahead. The leading and trailing edges of this uniform wavetrain are given by a simple phase and group velocity argument. This argument also predicts a minimum jump height cut-off for the uniform wavetrain to exist, which is found to be in

excellent agreement with numerical solutions. In general, excellent agreement was found between the derived analytical solutions and numerical solutions. This work is only a preliminary study of undular bores in nematic liquid crystals in the nonlocal regime. The wave structure linking the KdV bore to the uniform wavetrain ahead needs to be found, the amplitude of this wavetrain derived and a better description of the KdV bore for a non-small jump height needs to be found, among other matters. These further details are currently under investigation.

- [1] G.B. Whitham, *Linear and Nonlinear Waves*, J. Wiley and Sons, New York (1974).
- [2] P.G. Baines, *Topographic Effects in Stratified Flows*, Cambridge Monographs on Mechanics, Cambridge (1995).
- [3] R.S. Johnson, "A non-linear equation incorporating damping and dispersion," *J. Fluid Mech.*, **42**, 49–60 (1970).
- [4] G.B. Whitham, "A general approach to linear and non-linear dispersive waves using a Lagrangian," *J. Fluid Mech.*, **22**, 273–283 (1965).
- [5] G.B. Whitham, "Non-linear dispersive waves," *Proc. Roy. Soc. London A*, **283**, 238–261 (1965).
- [6] G.B. Whitham, "Variational methods and applications to water waves," *Proc. Roy. Soc. Lond. A*, **299**, 6–25 (1967).
- [7] J. Kevorkian and J.D. Cole, *Perturbation Methods in Applied Mathematics*, Springer-Verlag, New York (1981).
- [8] A.V. Gurevich and L.P. Pitaevskii, "Nonstationary structure of a collisionless shock wave," *Sov. Phys. JETP*, **33**, 291–297 (1974).
- [9] B. Fornberg and G.B. Whitham, "Numerical and theoretical study of certain non-linear wave phenomena," *Phil. Trans. Roy. Soc. Lond. Ser. A—Math. and Phys. Sci.*, **289**, 373–404 (1978).
- [10] H. Flaschka, M.G. Forest and D.W. McLaughlin, "Multiphase averaging and the inverse spectral solution of the Korteweg-de Vries equation," *Comm. Pure Appl. Math.*, **33**, 739–784 (1980).
- [11] G.A. El, V.V. Khodorovskii and A.V. Tyurina, "Determination of boundaries of unsteady oscillatory zone in asymptotic solutions of non-integrable dispersive wave equations," *Phys. Lett. A*, **318**, 526–536 (2003).
- [12] G.A. El, "Resolution of a shock in hyperbolic systems modified by weak dispersion," *Chaos*, **15**, 037103 (2005).
- [13] R.H.J. Grimshaw and N.F. Smyth, "Resonant flow of a stratified fluid over topography," *J. Fluid Mech.*, **169**, 429–464 (1986).
- [14] N.F. Smyth, "Modulation theory solution for resonant flow over topography," *Proc. Roy. Soc. Lond. A*, **409**, 79–97 (1987).
- [15] J.G. Esler and J.D. Pearce, "Dispersive dam-break and lock-exchange flows in a two-layer fluid," *J. Fluid Mech.*, **667**, 555–585 (2011).
- [16] N.F. Smyth and P.E. Holloway, "Hydraulic jump and undular bore formation on a shelf break," *Journal of Physical Oceanography*, **18**, 947–962 (1988).
- [17] R.H. Clarke, R.K. Smith and D.G. Reid, "The morning glory of the Gulf of Carpentaria: an atmospheric undular bore," *Monthly Weather Rev.*, **109**, 1726–1750 (1981).
- [18] D.R. Christie, "Long nonlinear waves in the lower atmosphere," *J. Atmos. Sci.*, **46**, 1462–1491 (1989).
- [19] V.A. Porter and N.F. Smyth, "Modelling the Morning Glory of the Gulf of Carpentaria," *J. Fluid Mech.*, **454**, 1–20 (2002).
- [20] T.R. Marchant and N.F. Smyth, "Approximate solutions for magmon propagation from a reservoir," *IMA J. Appl. Math.*, **70**, 796–813 (2005).
- [21] N.I. Gershenzon, V.G. Bykov and G. Bambakidis, "Strain waves, earthquakes, slow earthquakes, and afterslip in the framework of the Frenkel-Kontorova model," *Phys. Rev. E*, **79**, 056601 (2009).
- [22] N.K. Lowman and M.A. Hofer, "Dispersive shock waves in viscously deformable media," *J. Fluid Mech.*, **718**, 524–557 (2013).
- [23] N.K. Lowman and M.A. Hofer, "Fermionic shock waves: Distinguishing dissipative versus dispersive resolutions," *Phys. Rev. A*, **88**, 013605 (2013).
- [24] G.A. El, A. Gammal, E.G. Khamis, R.A. Kraenkel and A.M. Kamchatnov, "Theory of optical dispersive shock waves in photorefractive media," *Phys. Rev. A*, **76**, 053183 (2007).
- [25] M. Crosta, S. Trillo and A. Fratolocchi, "The Whitham approach to dispersive shocks in systems with cubic-quintic nonlinearities," *New J. Phys.*, **14**, 093019 (2012).

- [26] M. Crosta, A. Fratolocchi and S. Trillo, “Double shock dynamics induced by the saturation of defocusing nonlinearities,” *Opt. Lett.*, **37**, 1634–1636 (2012).
- [27] M. Conforti, F. Baronio and S. Trillo, “Resonant radiation shed by dispersive shock waves,” *Phys. Rev. A*, **89**, 013807 (2014).
- [28] J. Fatome, C. Finot, G. Millot, A. Armaroli and S. Trillo, “Observation of optical undular bores in multiple four-wave mixing,” *Phys. Rev. X*, **4**, 021022 (2014).
- [29] I.C. Khoo, *Liquid Crystals: Physical Properties and Nonlinear Optical Phenomena*, Wiley, New York (1995).
- [30] M. Peccianti and G. Assanto, “Nematicons,” *Phys. Rep.*, **516**, 147–208 (2012).
- [31] G. Assanto, *Nematicons, spatial optical solitons in nematic liquid crystals*, John Wiley and Sons, New York (2012).
- [32] A. Piccardi, A. Alberucci, N. Tabiryani and G. Assanto, “Dark nematicons,” *Opt. Lett.*, **36**, 1356–1358 (2011).
- [33] M. Peccianti, G. Assanto, A. De Luca, C. Umeton and I.C. Khoo, “Electrically assisted self-confinement and waveguiding in planar nematic liquid crystal cells,” *Appl. Phys. Lett.*, **77**, 7–9 (2000).
- [34] N. Ghofraniha, C. Conti, G. Ruocco and S. Trillo, “Shocks in nonlocal media,” *Phys. Rev. Lett.*, **99**, 043903 (2007).
- [35] C. Barsi, W. Wan, C. Sun and J.W. Fleischer, “Dispersive shock waves with nonlocal nonlinearity,” *Opt. Lett.*, **32**, 2930–2932 (2007).
- [36] A. Armaroli, S. Trillo and A. Fratolocchi, “Suppression of transverse instabilities of dark solitons and their dispersive shock waves,” *Phys. Rev. A*, **80**, 053803 (2009).
- [37] C. Conti, A. Fratolocchi, M. Peccianti, G. Ruocco and S. Trillo, “Observation of a gradient catastrophe generating solitons,” *Phys. Rev. Lett.*, **102**, 083902 (2009).
- [38] W. Wan, S. Jia and J.W. Fleischer, “Dispersive superfluid-like shock waves in nonlinear optics,” *Nature Phys.*, **3**, 46–51 (2007).
- [39] W. Wan, D.V. Dylov, C. Barsi and J.W. Fleischer, “Diffraction from an edge on a self-focusing medium,” *Opt. Lett.*, **35**, 2819–2821 (2010).
- [40] G. Assanto, T.R. Marchant and N.F. Smyth, “Collisionless shock resolution in nematic liquid crystals,” *Phys. Rev. A*, **78**, 063808 (2008).
- [41] T.R. Marchant and N.F. Smyth, “Semi-analytical solutions for dispersive shock waves in colloidal media,” *J. Phys. B: Atomic, Molec. and Opt. Phys.*, **45**, 145401 (2012).
- [42] G.A. El, V.V. Geogjaev, A.V. Gurevich and A.L. Krylov, “Decay of an initial discontinuity in the defocusing NLS hydrodynamics,” *Physica D*, **87**, 186–192 (1995).
- [43] G. Assanto, A.A. Minzoni, M. Peccianti and N.F. Smyth, “Optical solitary waves escaping a wide trapping potential in nematic liquid crystals: modulation theory,” *Phys. Rev. A*, **79**, 033837 (2009).
- [44] A. Alberucci, A. Piccardi, M. Peccianti, M. Kaczmarek, and G. Assanto, “Propagation of spatial optical solitons in a dielectric with adjustable nonlinearity,” *Phys. Rev. A*, **82**, 023806 (2010).
- [45] C. Conti, M. Peccianti and G. Assanto, “Route to nonlocality and observation of accessible solitons,” *Phys. Rev. Lett.*, **91**, 073901 (2003).
- [46] E.A. Kuznetsov and A.M. Rubenchik, “Soliton stabilization in plasmas and hydrodynamics,” *Phys. Rep.*, **142**, 103–165 (1986).
- [47] F.W. Dabby and J.R. Whinnery, “Thermal self-focusing of laser beams in lead glasses,” *Appl. Phys. Lett.* **13**, 284–286 (1968).
- [48] C. Rotschild, M. Segev, Z. Xu, Y.V. Kartashov and L. Torner, “Two-dimensional multipole solitons in nonlocal nonlinear media,” *Opt. Lett.* **31**, 3312–3314 (2006).
- [49] C. Rotschild, B. Alfassi, O. Cohen and M. Segev, “Long-range interactions between optical solitons,” *Nature Phys.* **2**, 769–774 (2006).
- [50] M. Segev, B. Crosignani, A. Yariv and B. Fischer, “Spatial solitons in photorefractive media,” *Phys. Rev. Lett.* **68**, 923–926 (1992).
- [51] A.B. Aceves, J.V. Moloney and A.C. Newell, “Theory of light-beam propagation at nonlinear interfaces. I Equivalent-particle theory for a single interface,” *Phys. Rev. A*, **39**, 1809–1827 (1989).
- [52] A. Cheskidov, D.D. Holm, E. Olson and E.S. Titi, “On a Leray- α model of turbulence,” *Proc. R. Soc. Lond. A* **461**, 629–649 (2005).
- [53] A. Ilyin, E.M. Lunasin and E.S. Titi, “A modified-Leray- α subgrid scale model of turbulence,” *Nonlinearity* **19**, 879–897 (2006).
- [54] R. Penrose, “Quantum computation, entanglement and state reduction,” *Phil. Trans. R. Soc. A*, **356**, 1927–1939 (1998).
- [55] Y.S. Kivshar, “Dark solitons in nonlinear optics,” *IEEE J. Quant. Electron.*, **29**, 250–264 (1993).

- [56] Y.S. Kivshar and B. Luther-Davies, “Dark optical solitons: physics and applications,” *Phys. Rep.*, **298**, 81–197 (1998).
- [57] T.P. Horikis, “Small-amplitude defocusing nematicons,” *J. Phys. A*, **48**, 02FT01 (2015).
- [58] T.R. Marchant and N.F. Smyth, “Approximate techniques for dispersive shock waves in nonlinear media,” *J. Nonlin. Opt. Phys. Mater.*, **21**, 1250035 (2012).
- [59] B.D. Skuse, “The Interaction and Steering of Nematicons,” Ph.D. thesis, University of Edinburgh (2010).
- [60] W.H. Press, S.A. Teukolsky, W.T. Vetterling, and B.P. Flannery, *Numerical Recipes in Fortran. The Art of Scientific Computing*, Cambridge University Press (1992).